LAWRENCE
LIVERMORE
NATIONAL
LABORATORY

LLNL-JRNL-443751

Algorithm for precision sub-sample timing between Gaussian like pulses

R. A. Lerche, B. P. Golick, J. P. Holder, D. H. Kalantar

July 20, 2010

Review of Scientific Instruments

Disclaimer

Algorithm for precision sub-sample timing between Gaussian like pulses[a)]

R. A. Lerche,[b)] B. P. Golick, J. P. Holder, and D. H. Kalantar

Lawrence Livermore National Laboratory, P. O. Box 808, Livermore, California 94551, USA

(Presented 19 May 2010; received XXXXX; accepted XXXXX; published online XXXXX)

Moderately priced oscilloscopes available for the NIF power sensors and target diagnostics have 6-GHz bandwidths at 20 to 25 GS/s (40 ps sample spacing). Some NIF experiments require cross timing between instruments be determined with accuracy better than 30 ps. A simple analysis algorithm for Gaussian-like pulses such as the 100-ps wide NIF timing fiducial can achieve single-event cross-timing precision of 1 ps (1/50 of the sample spacing). The midpoint-timing algorithm is presented along with simulations that show why the technique produces good timing results. Optimum pulse width is found to be ~2.5 times the sample spacing. Experimental measurements demonstrate use of the technique and highlight the conditions needed to obtain optimum timing performance.

I. BACKGROUND

Target experiments at the National Ignition Facility (NIF) use 192 laser beams to heat and compress small fuel-filled capsules to create fusion reactions.[1] Detailed measurements of the laser and target plasma characteristics associated with an experiment are collected with a variety of instruments, each with its own recording system. If we understand the physical processes occurring in a target, models of the experiment should accurately predict the characteristics that are observed and measured. Time is an important parameter for many measurements. How well are the beams synchronized? When are radiations such as x rays and neutrons emitted relative to the laser beams striking the target? Temporal information is often recorded with oscilloscopes and streak cameras. Experimental requirements often specify timing accuracies of a few 10s of picoseconds.

The timing fiducial is an important concept for cross-timing the time bases of many seemingly independent instruments.[2] At NIF timing pulses (timing fiducials) start from a common source, a single, nominally Gaussian 100-ps (FWHM), 1.05-μm laser pulse. The fiducial system amplifies and splits the initial pulse into multiple pulses that can be further amplified, split, frequency shifted, and transported to recording instruments located throughout the large facility. As long as the optical path between the common "seed" pulse and each instrument receiving a fiducial pulse remains fixed, the temporal relationship between fiducials received at the different recording devices remains fixed. Calibration experiments determine the temporal relationship between instrument time bases and the arrival of laser pulses at target chamber center (TCC). Once calibrated, the shift of the time base of an instrument can be made during analysis so that the measured phenomena can be related to the time each laser beam reached TCC and irradiated the target. The NIF fiducial pulse is synchronized with the 48 quad pulses. Each quad pulse is split 4 ways to produce the 192 NIF beams. The fiducial and each quad are independently triggered and have ~10 ps of uncorrelated jitter. Although fiducial jitter relative to the laser beams is very small, this is not a requirement for good cross timing of time bases on a single experimental shot. If the fiducial timing changes on one instrument, it changes the same amount on all the other instruments thus maintaining the cross-timing relationships. Low jitter, however, is necessary when the fiducial is used to establish correct instrument timing prior to a shot.

Temporal measurements are generally recorded with one of two instruments: an oscilloscope or a streak camera. Fast streak cameras[2,3] generally produce measurements with better single-shot bandwidth and have an additional spatial dimension. Oscilloscopes, however, are less expensive, can be couple to more sensitive transducers, and are easier to implement. The temporal resolution of an oscilloscope is Nyquist limited at twice the sample spacing of the time base. The time of a recorded event, however, can be determined with much better precision. In this paper we describe a simple algorithm for defining the time of a sparsely sampled Gaussian pulse with a precision that is 1/50 of the sample spacing. The method allows a narrow (100 ps) pulse recorded with a 6-GHz, 25 GS/s (40 ps per sample) oscilloscope to be timed with 1-ps precision on a single-shot basis. Simulations show why the technique works, and experimental measurements demonstrate the power of the algorithm.

II. MIDPOINT TIMING

Consider as an example an 80-ps FWHM Gaussian pulse sampled every 40 ps. The sparsely sampled pulse can take on a variety of shapes. Figure 1 shows such a pulse with the sampling point at the peak and at offsets from the peak of 5, 10, 15, and 20 ps. The recorded pulse shape depends on timing of the sampling grid relative to the pulse peak. When a sampling point occurs at t = 0, the pulse has a sharp peak with maximum amplitude. If the sampling point is offset by 20 ps, the pulse has a 40-ps wide flat top and reduced amplitude. For other offsets, the recorded pulse has an asymmetric, but predictable shape in the absence of noise.

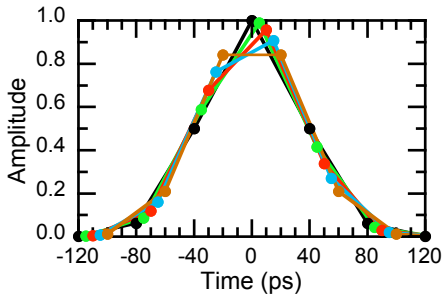

Figure 1. 80-ps Gaussian pulses sampled every 40 ps. Shape depends on sampling time relative to pulse peak.

[a)]Contributed paper published as part of the Proceedings of the 18th Topical Conference on High-Temperature Plasma Diagnostics, Wildwood, New Jersey, May, 2010.

[b)]lerche1@llnl.gov.

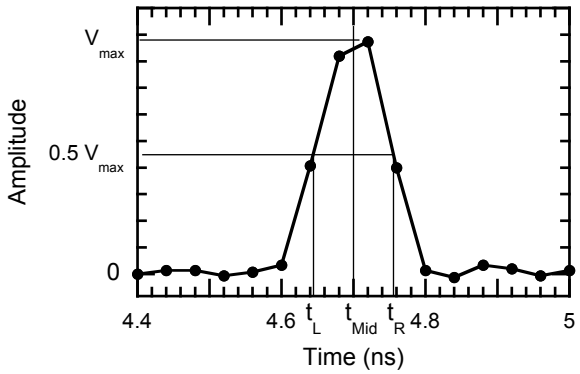

Figure 2. Midpoint analysis. Method uses time t_{Mid} midway between half-maximum times t_L and t_R as time of the peak.

A simple analysis technique that we call midpoint timing allows an accurate determination for the time of the pulse peak. Figure 2 illustrates the algorithm. Start by establishing the signal baseline as y = 0. In the absence of noise, this is an easy task. When noise is present, the flat region to either side of the pulse is used to estimate y = 0 and the noise level. Next, find the peak amplitude for the pulse. This is simply the amplitude of the sample point with the greatest magnitude, y_{max}. Now, moving outward from the peak, use linear interpolation to find the first instance when the pulse amplitude reaches the half-maximum level on leading and trailing edges of pulse (i.e. times t_L and t_R where $y = 0.5*y_{max}$). Finally, define the time of the pulse as the midpoint between half-maximum points: $t_{Mid} = 0.5*(t_L + t_R)$. The subscripts L, R, and Mid stand for **L**eft, **R**ight and **Mid**point.

Computer simulations show that the simple algorithm described in the preceding paragraph is a powerful tool for finding pulse times with an accuracy that is a small fraction of the sample spacing. The simulations use Gaussian pulses with FWHMs that range between 40 and 400 ps in 1 ps steps. The peak of each pulse is initially centered on a sampling point. Then, for each FWHM, the sampling grid is shifted in 0.8-ps increments across the pulse. This provides a fine measurement of the effect of sampling grid offset relative to the true center of the pulse. Figure 3 shows the timing shifts for t_L, t_R, and t_{Mid} versus sampling offset for 3 selected pulse widths: 64, 80, and 105 ps. In each case, the leading and trailing half-maximum times compensate each other to form a much more accurate midpoint time.

Average characteristics that can be measured for each pulse width are obtained by averaging over all possible sampling offsets. The average and standard deviation are calculated for midpoint time, width, and amplitude. The expected jitter (standard deviation in pulse midpoint time) as a function of pulse

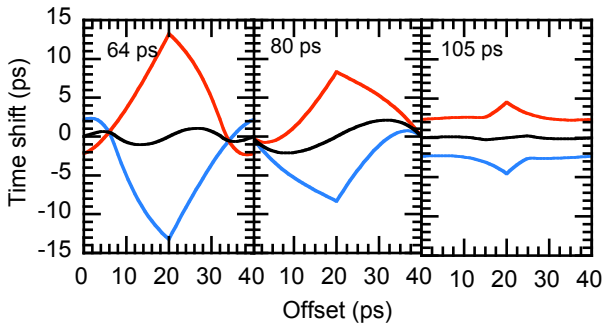

Figure 3. Shift in half-max and midpoint times for selected pulse widths. t_R upper, t_L lower, and t_{Mid} middle curve.

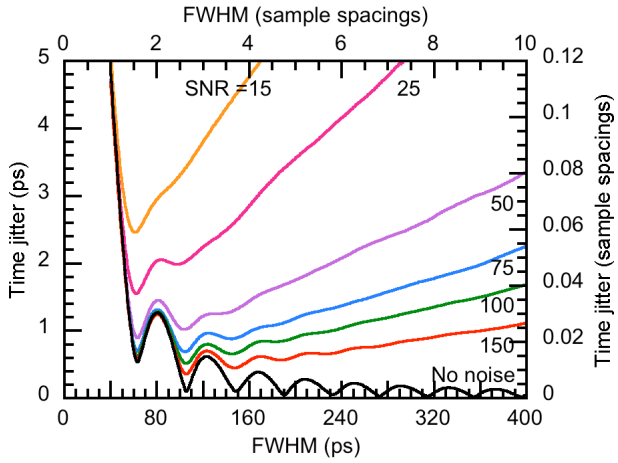

Figure 4. Time jitter versus pulse width for various SNRs. Width and jitter are given in ps and in sample spacings.

width is plotted in Fig. 4. Jitter increases greatly for pulse widths narrower than 60 ps. There is too little sampling with the 40 ps sample spacing for the leading and trailing pulse edges to effectively compensate each other at all offsets. For pulses wider than 60 ps, leading and trailing edge compensation is very good when there is no noise present. Jitter shows an oscillation with the first two local minima of < 1 ps at pulse widths of 63 and 106 ps with a local maximum of 1.5 ps for a pulse width of 80 ps. Jitter is less than 1 ps for pulse widths greater than 100 ps.

A temporally uniform noise is added to the simulation to produce a more realistic estimate for laboratory-measured signals, The additive noise corresponds to oscilloscope and photodiode amplifier noise and assumes each signal sample point has enough statistical content so that the signal shot noise is negligible. For a pulse of amplitude 1, noise for each sample point is randomly selected from a Gaussian distribution whose standard deviation σ_{noise} is 1/SNR, where SNR is the signal-to-noise ratio. For each 1-ps sampling offset, 50 pulses with random noise applied were generated and analyzed. At each pulse width the standard deviation of the timing is the average of 2500 pulses. Estimated jitter with noise applied is also shown in Fig. 4 for selected signal-to-noise ratios between 15 and 150. When the SNR is greater than ~75, sub picosecond jitter can be achieved with pulse widths between 100 and 160 ps.

While the midpoint-timing algorithm produces good timing results, measurements of pulse width and amplitude can have significant error. Figure 5 shows the FWHM and amplitude as a function of the sampling offset for several pulse widths. Maximum error occurs at an offset of 20-ps and decreases with increasing pulse width. The average and standard deviation of the

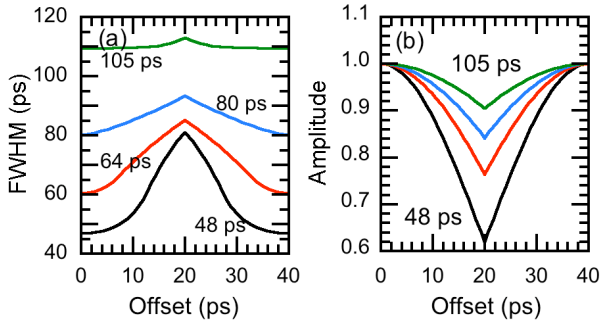

Figure 5. FWHM and amplitude versus sampling offset for selected pulse widths of 48, 64, 80, and 105 ps.

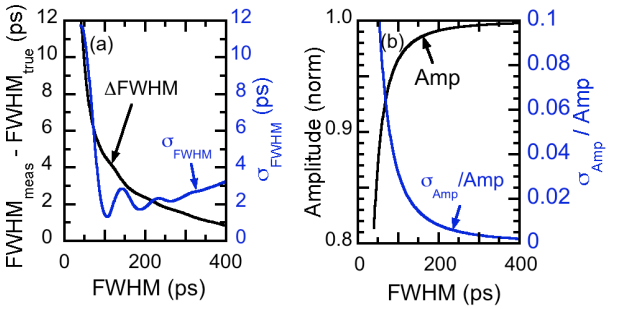

Figure 6. Expected average and standard deviation for FWHM and amplitude versus pulse width. (a) FWHM, (b) amplitude.

FWHM and amplitude are easily measured quantities that help demonstrate the effectiveness of midpoint timing. Figure 6a shows the expected widening of the measured FWHM and its standard deviation versus pulse width. Figure 6b shows the expectation value of the measured amplitude and its standard deviation versus pulse width. A demonstration of the pulse jitter capability of the algorithm should also be consistent with the pulse characteristics presented in Figs. 4 through 6.

III. JITTER MEASUREMENTS

Figure 7 shows the experimental setup used to demonstrate the precision of jitter measurements made using the midpoint-timing algorithm. A nominally 100-ps wide Gaussian, 1.05-μm laser pulse propagating through a single-mode optical fiber is split into three separate pulses. Two of the pulses are recombined after one of them has been delayed by propagation through an extra length of fiber. The pulse pair is detected by a 25-GHz New Focus 1431 photodetector[4] and converted into electrical pulses that are recorded by one channel of a 6-GHz 25-GS/s Tektronix DPO70604 digitizer.[5] The two pulses of this pulse pair are nominally identical in width, amplitude, and jitter. Their time separation caused by a passive optical fiber remains constant throughout the experiments. The third pulse, which passes through an optical attenuator, is detected by an amplified 10-GHz TIA-3000 optical-to-electrical (O/E) converter[6] and recorded on a second channel of the digitizer. The attenuator changes pulse amplitude allowing the effect of SNR to be demonstrated.

Data were recorded in 6 groups of 25 shots. Each group had a different attenuator setting so that the amplitude of pulse 3 ranged from 250 to 1,500 mV in steps of 250 mV. The average time separation between pulses 1 and 2 for the 150 shots is 5,255.191 ps with a jitter between group averages of 0.038 ps. Measured jitter between pulses 1 and 2 for all 150 shots is 0.601 ps. Assuming the two pulses are identical, the jitter contributed by each pulse is 0.425 ps ($0.601/2^{1/2}$). The jitter between pulses 1 and 3 ranged from 0.62 to 0.90 ps and depends on pulse 3 amplitude. After correction for pulse 1 jitter, pulse 3 jitter ranges from 0.48 to 0.80 ps. The same jitter is observed between pulses 2 and 3. Samples of the three pulses are shown in Fig. 8.

Measured data compared with simulations demonstrates the power of midpoint timing. First consider pulses 1 and 2.

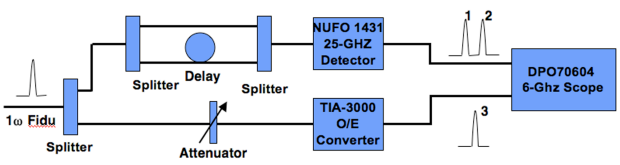

Figure 7. Experimental setup.

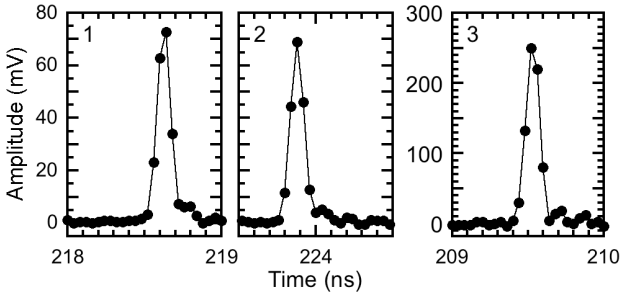

Figure 8. Sample data set. Pulse 3 is from the 250 mV group

Simulations show that measured widths will be larger than the true width. So the first step for comparing measured quantities with simulations is to establish the true pulse width. Measured widths for pulses 1 and 2 are 106.65 ps. This corresponds to an actual width of 102 ps (see Fig. 9a). Measured widths for pulse 3 range from 110 to 115 ps depending on amplitude. At the highest amplitude the O/E converter becomes nonlinear resulting in some pulse broadening. At the two extremes, the true pulse widths are ~105.5 and 110 ps. Using these values of FWHM, the measured standard deviations for FWHM and amplitude are plotted on simulation curves showing the expected values in Figs. 9b and 9c. Finally, measured jitter for all pulses is plotted in Fig. 10 along with corresponding SNR simulations.

Another demonstration of the simulation accuracy is a measurement of pulse width and amplitude versus offset. Figure 11a shows the measured width for 250 pulses (1 and 2) versus timing offset along with the expected FWHM determined by simulation. The data is a good match to the simulation. Figure 11b shows measured amplitude normalized to the average amplitude versus timing offset compared with simulation. The simulation accurately predicts amplitude. An amplitude check like this is only possible when shot-to-shot amplitude is very stable.

IV. DISCUSSION

Simulations and experimental measurements presented in this article achieve better than 1 ps jitter with a 25-GS/s sampling

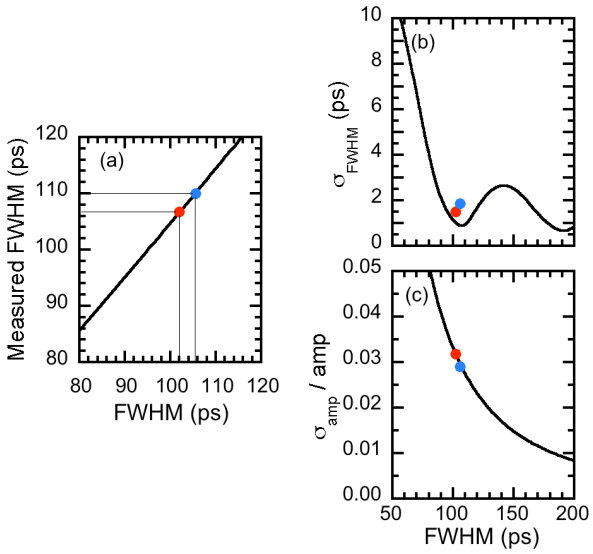

Figure 9. Measured pulse characteristics compared with simulations. Solid curves are the simulations, dots are the measured values. (a) Measured FWHM versus true FWHM, (b) σ_{FWHM} versus FWHM, and (c) σ_{Amp} / Amp versus FWHM.

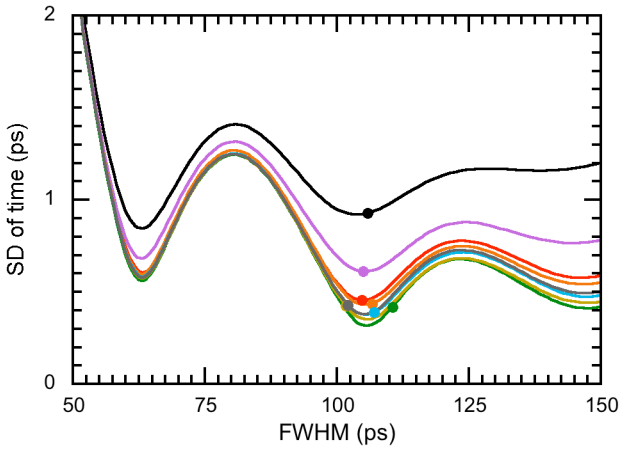

Figure 10. Measured jitter for various SNRs compared with simulations. Points represent measurements; curves represent simulations of jitter versus pulse width. Pulses 1 and 2 with widths of 102 ps have an SNR of 135. Pulse 3 widths vary from 105 to 110 ps and have SNRs ranging from 55 to 163.

rate (40-ps sample spacing). This shows that the time when a short pulse occurs can be determined with a precision that is 1/50 of the sample spacing using midpoint timing. It is important to realize that the plots presented in this article are applicable to all sampling rates when their time axes are converted from ps to units of sample spacing. This is demonstrated in Fig. 4 where double x and y axes are used (one xy pair is in time units of ps, the other in time units of sample spacings). To convert plots presented in this article into units of sample spacing, just divide each time axis value by the 40 ps/sample spacing.

There are three pulse and recorder conditions that must be met to achieve the best possible cross timing between instrument time bases. First, the cross-timing pulse (fiducial) directed to the two separate recorders should be derived from one common source pulse that is split and distributed over a fixed set of passive elements. This eliminates any jitter associated with synchronizing independent pulses. Second, select a nominally Gaussian-shaped pulse whose width is ~2.5 times the sample spacing. A Gaussian pulse has been shown to work well for achieving good midpoint timing; other pulse shapes not explored in this paper may also work and can be evaluated using relatively easy simulations. Finally, signals should be recorded with the best possible SNR. Figure 4 shows that <1 ps jitter is achieved for pulse widths between 100 and 160 ps when the SNR is >75 and the signal is sampled every 40 ps.

A fiducial pulse should be stable in shape and amplitude. If the pulse is slightly asymmetric, a variation in shot-to-shot width may produce a width-dependent walk of the midpoint time. This should not have an impact on cross timing, but may affect shot-to-shot comparisons. Some variation in pulse amplitude can be tolerated. There are, however, two amplitude related conditions to avoid. A significant drop in amplitude will result in poorer SNR and thus increase jitter, and a significant increase in amplitude may send the detector or recording system into a nonlinear operating range that distorts the pulse shape and impacts the timing. Stable amplitude is preferred.

Pulse jitter depends on pulse quality. Several metrics have been presented that monitor pulse quality. Before measured data can be compared with simulations, two simulation parameters must be determined: the true pulse width and the SNR. Measured pulse width can easily be converted to the true pulse width based on simulations presented in Fig. 6. Noise σ_{noise} is measured as the

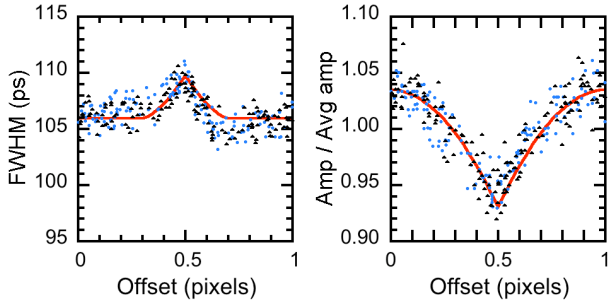

Figure 11. Comparison of measurements with simulations for 102-ps wide pulse. (a) FWHM verses offset. (b) Amplitude versus FWHM.

standard deviation of the signal trace in a region where there is no signal, and SNR is approximately the average pulse amplitude divided by the noise. Then the following pulse characteristics can be compared with simulations: FWHM vs time offset, amplitude versus time offset, standard deviation of the FWHM and standard deviation of the amplitude. When these quantities fail to agree with simulation, it is an indication that there may be a problem with the fiducial pulse shape.

It is not necessary to know the precise pulse shape for midpoint analysis to work. Shape, however, should be stable. Also, it is unnecessary for the pulse to be perfectly symmetric. Great results can be obtained even if pulse is slightly asymmetric. For significantly non-Gaussian or asymmetric pulses, it is worthwhile doing a simulation of the specific pulse shape. Deviations from symmetry can be detected with experimental data using plots of FWHM and amplitude versus sampling offset (like Fig. 11). For a symmetric pulse, peak fwhm and minimum amplitude occur at an offset halfway between sampling points and shape is very predictable. Location of the peak fwhm and minimum amplitude will shift towards one of the sampling points when pulse is asymmetric. A slight asymmetry in Fig. 11a shows the pulse used in the example to be slightly non-Gaussian.

ACKNOWLEDGMENTS

A special thank you to Zachariah C. Sober for acquiring the experimental data and to Donald F. Browning for providing lab space and setting up the optical test bed. This work performed under the auspices of the U.S. Department of Energy by Lawrence Livermore National Laboratory under Contract DE-AC52-07NA27344.

[1]E. I. Moses, R. N. Boyd, B. A. Remington, C. J. Keane, and R. Al-Ayat**,** Phys. Plasmas **16**, 041006 (2009).
[2]R. A. Lerche, SPIE Vol. 1346 Ultrahigh- and High-Speed Photography, Videography, Photonics, and Velocimetry '90, 376 (1991).
[3]W. R. Donaldson R. Boni, R. L. Keck, and P. A. Jaanimagi, Rev. Sci. Instrum., **73**, 2606 (2002).
[4]New Focus, a Newport Corporation brand, Newport Corporation, 1791 Deere Ave., Irvine, CA 92606.
[5]Tektronix, Inc., P.O. Box 500, Beaverton, OR 97077.
[6]Terahertz Technologies, Inc., 169 Clear Road, Oriskany, NY 13424.